NASA TECHNICAL NOTE **NASA TN D-4519**

C. 1

NASA TN D-4519

FEASIBILITY STUDY OF OPTIMUM ON-OFF ATTITUDE CONTROL SYSTEM FOR SPACECRAFT

by John D. Regetz, Jr., and Thomas M. Nelson

Lewis Research Center
Cleveland, Ohio

NATIONAL AERONAUTICS AND SPACE ADMINISTRATION • WASHINGTON, D. C. • APRIL 1968

FEASIBILITY STUDY OF OPTIMUM ON-OFF ATTITUDE CONTROL SYSTEM FOR SPACECRAFT

By John D. Regetz, Jr., and Thomas M. Nelson

Lewis Research Center
Cleveland, Ohio

NATIONAL AERONAUTICS AND SPACE ADMINISTRATION

For sale by the Clearinghouse for Federal Scientific and Technical Information
Springfield, Virginia 22151 – CFSTI price $3.00

FEASIBILITY STUDY OF OPTIMUM ON-OFF ATTITUDE CONTROL SYSTEM FOR SPACECRAFT

by John D. Regetz, Jr., and Thomas M. Nelson

Lewis Research Center

SUMMARY

Attitude control of orbiting spacecraft is generally performed in an on-off mode; no corrective thrust is provided until a preset angular error is obtained. For a given disturbance torque, the phase-plane trajectory then depends on the size of the angular impulse imparted during thrusting. For comparatively large angular impulses, the trajectory contacts both deadband limits alternately; for small impulses, the disturbance reverses the spacecraft angular rate before it can contact one side of the deadband. If the thrustor firing time is controlled, a limit cycle can be obtained in which the maximum angular excursion within the deadband is such that the spacecraft just misses contacting the opposite deadband limit. The fuel consumption is then minimum because a single-sided trajectory is maintained, and the number of thrust pulses during a given control period is minimized because the time between firings is a maximum.

A single-axis control system that provides this optimum trajectory was functionally designed and investigated by simulation on an analog computer. The system calculates spacecraft angular velocity and acceleration at the deadband limit, and determines the thrustor "on" time which produces the optimum trajectory. The system was investigated with such varying degrees of sophistication as the inclusion of compensation for the effects of a slow time rate of change of disturbance torque. The various simulated system configurations were subjected to sinusoidal disturbance torques of varying amplitudes. A simulated, conventional, nonoptimum system was subjected to the same disturbances and the results compared.

The optimum system reduces the average thrustor pulsing frequency for all configurations studied by as much as 10^6 pulses per year over the nonoptimum system. The total thrustor on time in seconds per year (a measure of the fuel consumption) is virtually identical for all configurations of the optimum system and for the nonoptimum system, which indicates that both systems operated in a one-sided limit cycle most of the time and, thus, had nearly minimum fuel consumption. The circuit for calculating the time rate of change of the disturbance torque appears to be the most difficult portion of

the system to implement in hardware, and this fact may outweigh any advantage to its inclusion in the system.

INTRODUCTION

Of particular importance in the attitude control of unmanned spacecraft is the requirement that control systems operate reliably without maintenance over long periods of time and that they be of minimum size and weight. The type of system that best fulfills these requirements is one in which both the energy consumption rate and the number of cycles of operation are kept at a minimum.

Attitude control systems designed according to the momentum discharge principle are most generally operated in an on-off rather than a proportional fashion, principally because of the added difficulty and complexity in modulating the thrust level. As a consequence of this on-off operation, the vehicle drifts back and forth within a specified angular error or deadband. Measured or derived vehicle rate information is usually added to stabilize the resulting limit cycle in the presence of external disturbances. The vehicle motion in the limit cycle is then a function not only of the external disturbing torques, but also of the control system parameters. In particular, the ratio of rate to position information in the thrustor on-off signal is usually adjusted to control the limit cycle characteristics.

In the absence of any disturbance torques, the limit cycle traversed in the phase plane by the spacecraft will be "hard", that is, the spacecraft alternately contacts the positive and negative deadband limits, traversing the deadband with constant angular velocity. A fixed angular impulse is imparted to the vehicle at either deadband limit to reverse the rate. Under these conditions, both the energy used, as manifested by the fuel consumption, and the number of cycles of operation, as shown by the thrustor pulsing frequency, are direct functions of the magnitude of the angular impulse imparted to the spacecraft. This impules, in turn, is fixed by the control system parameters.

If a constant disturbance torque is exerted on the spacecraft, it tends to operate more on one side of the deadband than on the other. If the control angular impulse is sufficiently small, the disturbance torque will reverse the vehicle angular rate before it contacts the opposite deadband limit, which results in one-sided or "soft" limit cycle operation. Here, the spacecraft successively contacts only one deadband limit. The fuel consumption then depends on the magnitude of the disturbance torque alone, and the pulsing frequency is inversely proportional to the time between firings, which in turn is a direct function of the magnitude of the control impulse. Minimum fuel consumption and pulsing frequency can be maintained for a given disturbance torque by adjusting the magnitude of the angular impulse delivered during thrustor firing as a function of the vehicle state existing at the deadband limit, so that the maximum excursion is obtained during coast without contacting the opposite limit. The required control impulse for this optimum limit cycle is then a function of the values of vehicle angular rate and disturbance torque, and of the derivatives of disturbance torque, which exist at the deadband.

A spacecraft attitude control system can be designed to operate in this optimum fashion with the use of attitude error as the only measured parameter This report describes the arrangement and computer investigation of such a control system.

SYMBOLS

d_a	duty cycle, dimensionless
F	thrust, lb; N
h	switching line hysteresis, rad
I_{sp}	specific impulse, (lb)(sec)/lb; (N)(sec)/kg
J	moment of inertia, $(slug)(ft^2)$; $(kg)(m^2)$
k_ϵ	constant factor used in calculating t_ϵ
l	thrustor moment arm, ft; m
N_f	total number of thrust pulses, dimensionless
P	total period of control, sec
S	Laplace transform variable, rad/sec
T_f	total thrustor on time, sec/yr
t	time, sec
t_ϵ	thrust-variation compensation time, sec
$\left.\begin{matrix} t_{\theta_1}, t_{\theta_2}, t_{\theta_3}, \\ t_{\theta_4}, t_{\theta_d} \end{matrix}\right\}$	times at which switching lines 1, 2, 3, 4, and θ_d are crossed, sec
$t_{\theta_3 -h}, t_{\theta_d -h}$	times at which negative half-switching lines are crossed, sec
t_1, t_2, t_3, t_0	time intervals as defined in fig. 1, sec
W	total fuel requirement, lb; kg
$\dot{w}$	fuel flow, lb/sec; kg/sec
α	ratio of peak disturbance torque to control torque
θ	spacecraft angular position, rad

θ_d	deadband limit or switching line angular position as defined in fig. 1, rad
$\dot{\theta}_d$	desired value of deadband reentry rate, rad/sec
θ_{max}	maximum angular excursion during coast in "soft" limit cycle, rad
θ_r	spacecraft angular position at thrustor shutoff, rad
$\dot{\theta}'_r$	angular rate as defined in fig. 6
$\left.\begin{matrix}\theta_1, \theta_2, \\ \theta_3, \theta_4\end{matrix}\right\}$	switching line angular position as defined in fig. 1, rad
$\left.\begin{matrix}\dot{\theta}_1, \dot{\theta}_2, \\ \dot{\theta}_3, \dot{\theta}_0\end{matrix}\right\}$	calculated angular rates as defined in fig. 1, rad/sec
$\Delta\theta$	angular intervals as defined in fig. 1, rad
λ	ratio of disturbance torque to moment of inertia, rad/sec^2
λ_c	ratio of control torque to moment of inertia, rad/sec^2
$\Delta\lambda$	correction term for nonzero $\dot{\lambda}$, rad/sec^2
σ_{av}	average percent deviation
τ_1	lead time constant in backup system, sec
τ_2	lag time constant in backup system, sec
ω_o	angular frequency, rad/sec

Subscripts:

b	backup system
c	coast
d	primary system
dl	delay
j	index of summation for feedback term
off	off time
on	on time
SGN	algebraic sign

Superscripts:

.	derivative with respect to time
'	corrected value

ANALYSIS

The phase-plane trajectory that minimizes both the fuel consumption and the pulsing frequency of an on-off attitude control system operating in the presence of external disturbance torques is that which allows the maximum angular excursion during the coast following a thrusting period, without contacting the opposite switching line (see the appendix). The property of such a trajectory is that the vehicle angular rate at thrustor shutoff $\dot{\theta}_r$ required to produce a given maximum excursion θ_{max} is a function of the disturbance torque,

$$\dot{\theta}_r = \int_0^{t_c/2} \lambda \, dt = \int_{\theta_r}^{\theta_{max}-\theta_r} \lambda \left(\frac{dt}{d\theta}\right) d\theta \tag{1}$$

For a constant disturbance torque, the rate at the deadband limit following thrustor shutoff relates to the maximum excursion by

$$\dot{\theta}_d = \sqrt{2\theta_{max}\lambda} \tag{2}$$

Thus, an orientation control system that commands an angular impulse each time the deadband is exceeded that in turn causes the vehicle angular rate at deadband reentry to satisfy equation (2) would operate in an optimum fashion, if θ_{max} were set equal to $2\theta_d$.

Actually, the thrustor shutoff results from a predetermined calculation rather than from a deadband reentry, as will be shown. Therefore, shutoff will not always occur right at the deadband limit. If the ratio of the control torque to the disturbance torque is large, however, the error that results from making this assumption is small. In any case, the chance of hitting the opposite switching line as a result of a difference between the actual thrust shutoff angle and the deadband limit can be minimized by setting θ_{max} at some major fraction of the total deadband width, thus allowing some angular margin. The resulting trajectory will still be nearly optimum. For the present study, θ_{max} was set at 0.9 of the total deadband width, or $1.8\,\theta_d$.

Basic System

The operation of the basic optimum system may be visualized by referring to the phase-plane representation presented in figure 1. As the vehicle coasts toward the positive deadband limit θ_d, the time required to traverse each of three angular intervals $\Delta\theta$ is measured and recorded:

$$\left.\begin{aligned} t_1 &= t_{\theta_3} - t_{\theta_1} \\ t_2 &= t_{\theta_4} - t_{\theta_2} \\ t_3 &= t_{\theta_d} - t_{\theta_3} \end{aligned}\right\} \tag{3}$$

The recorded times are then used to calculate from the following relations the vehicle angular rate and acceleration, and the thrustor on time:

$$\dot{\theta}_i = \frac{\Delta\theta}{t_i} \qquad i = (1, 3) \tag{4}$$

$$\lambda = \frac{(\dot{\theta}_3 - \dot{\theta}_1)}{t_2}$$

$$t_{on} = \frac{\dot{\theta}_3}{|\lambda_c|} + \frac{\sqrt{2\theta_{max}\lambda}}{|\lambda_c|} \tag{5}$$

The first term on the right side of equation (5) represents the thrusting time required to null the deadband exit rate. The second term follows from equation (2) and represents the thrusting time required to obtain an angular velocity at thrust off which will provide an angular excursion of θ_{max} during the following coast phase, for a constant disturbance torque. The absolute value of λ_c is taken so that t_{on} is a positive quantity. This operational method defines the basic optimum on-off control system.

Upgraded System

The basic system requires that the disturbance torque remain constant over at least one-half of a control cycle to maintain near optimum performance. However, it is possible to upgrade the system by calculating the expected change in the ratio of disturbance torque to inertia λ during the next half cycle to allow for time-varying disturbance torques. Assuming a constant time rate of change of disturbance torque yields

$$\theta_d - \theta_3 = \dot{\theta}_2 t_3 + \frac{1}{2}\lambda t_3^2 + \frac{1}{6}\dot{\lambda} t_3^3$$

from which

$$\dot{\lambda} = \frac{6(\dot{\theta}_3 - \dot{\theta}_2)}{t_3^2} - \frac{3\lambda}{t_3} \tag{6}$$

Therefore, the change in λ over the next one-half coast period is

$$\Delta\lambda = \dot{\lambda}\frac{t_c}{2} \cong \dot{\lambda}\sqrt{\frac{2\theta_{max}}{\lambda}} \tag{7}$$

Thus, for the upgraded system

$$t_{on} = \frac{\dot{\theta}_3}{|\lambda_c|} + \frac{\sqrt{2\theta_{max}\lambda'}}{|\lambda_c|} \tag{8}$$

where

$$\lambda' = \lambda + \Delta\lambda$$

System Compensation

The performance of both the basic and upgraded systems may be improved by adding terms to compensate for certain effects that cause a real or effective change in the value of the ratio of control torque to inertia λ_c. The first of these effects to be considered is the existence of the disturbance torque, during any given thrustor firing, which causes an apparent change in the control torque. Compensation for this effect is easily implemented by substituting the quantity $|\lambda_c| - |\lambda|$ for $|\lambda_c|$ in equations (5) and (8), or, alternatively, by multiplying the expression for t_{on} by the term $1 + (|\lambda|/|\lambda_c|)$. For ease in the computer simulation, the second method was used in this investigation.

A long-term variation in the characteristics of the thrustor will also lead to a change in the value of the control torque-to-inertia ratio. To maintain optimum system performance in the event of any such changes in the thrustor system behavior, a feedback may be added to the system to compare the actual vehicle rate at or near deadband reentry with the desired rate. As the vehicle reenters the deadband, the time to traverse the interval $\left(t_{\theta_d - h_d}\right) - \left(t_{\theta_3 - h_d}\right)$ is measured as before

$$t_0 = t_{(\theta_3 - h_d)} - t_{(\theta_d - h_d)} \tag{9}$$

Thus

$$\dot{\theta}_0 = \frac{\Delta\theta}{t_0} \tag{10}$$

For any given thrustor firing, the desired reentry velocity for the basic system is

$$\dot{\theta}_d = \sqrt{2\theta_{max}\lambda} \tag{11}$$

Therefore, an error in the thrustor on time for any given thrustor firing is represented by

$$t_{\epsilon, j} = \frac{\sqrt{2\theta_{max}\lambda}}{|\lambda_c|} - \frac{\dot{\theta}_0}{|\lambda_c|} \qquad j = (1, n) \tag{12}$$

The feedback term is then generated by a successive summation of the individual values of the error in the thrustor on time modified by a constant factor k_ϵ over all firings of a given thrustor:

$$t_\epsilon = \sum_j k_\epsilon t_{\epsilon, j} \qquad 0 \le k_\epsilon \le 1 \tag{13}$$

The development of the feedback term for the upgraded system is identical to that for the basic system with λ' substituted for λ in equation (12). Incorporating both of these compensation terms into the thrustor on time equations yields for the basic system,

$$t_{on} = \left(\frac{\dot{\theta}_3}{|\lambda_c|} + \frac{\sqrt{2\theta_{max}\lambda}}{|\lambda_c|} + t_\epsilon\right)\left(1 + \frac{|\lambda|}{|\lambda_c|}\right) + t_{dl} \tag{14}$$

and for the upgraded system,

$$t_{on} = \left(\frac{\dot{\theta}_3}{|\lambda_c|} + \frac{\sqrt{2\theta_{max}\lambda'}}{|\lambda_c|} + t_\epsilon\right)\left(1 + \frac{|\lambda|}{|\lambda_c|}\right) + t_{dl} \tag{15}$$

The t_{dl} term is added to the thrustor on time equations to allow for any comparatively short, known, time delay, such as electric engine warmup which is inherent in the thrustor system operation.

Disturbance-Torque Reversal and Backup System

An inspection of equations (14) and (15) reveals the possibility of obtaining a value under the radical which is less than 0, because λ may have reversed sign since the last thrustor firing. To avoid this computational difficulty, the t_{on} equations are written as follows:

$$t_{on} = \left(\frac{\dot{\theta}_3}{|\lambda_c|} + \frac{\sqrt{2\theta_{max}|\lambda|}}{|\lambda_c|} \text{SGN } \lambda + t_\epsilon\right)\left(1 + \frac{|\lambda|}{|\lambda_c|}\right) + t_{dl} \tag{14a}$$

$$t_{on} = \left(\frac{\dot{\theta}_3}{|\lambda_c|} + \frac{\sqrt{2\theta_{max}|\lambda'|}}{|\lambda_c|} \text{SGN } \lambda' + t_\epsilon\right)\left(1 + \frac{|\lambda|}{|\lambda_c|}\right) + t_{dl} \tag{15a}$$

These equations now permit the possibility of a negative value of t_{on}. A negative value indicates that the disturbance torque is of sufficient magnitude and in the proper direction to reverse the spacecraft angular velocity without the aid of a thrust pulse. Under these conditions, the thrustor is prohibited from firing. To prevent complete loss of control in the event that the disturbance torque direction reverses after the vehicle has crossed the deadband limit, or that the torque magnitude becomes larger than the primary system design can handle, a backup system must be provided. This system switches the thrustors both on and off by way of switching lines, as in a standard on-off system.

System Summary

The basic system calculates the thrustor on time required to produce a nearly optimum coast trajectory, assuming a constant disturbance torque. The upgraded system permits operation with a varying disturbance torque by estimating the average value of disturbance over the following coast half-cycle, and calculating the required thrusting time. In addition, compensation terms can be added to either system to minimize the effects of the disturbance torque canceling a portion of the control torque and of a slow variation of the control torque with time. Finally, a conventional on-off backup system is provided to maintain control for disturbances outside the design range.

Identical control systems are provided for both the positive and negative deadband limits, and these systems control the negative- and positive-oriented thrustors, respectively. The block diagram of the control system is presented in figure 2.

COMPUTER STUDY

The single-axis attitude control of a spacecraft with the system described in the previous section was simulated on an Electronic Associates, Incorporated, 231R-V analog computer. The simulation utilized the memory-logic capability of this machine to perform the required discontinuous operations. The computer was programmed so that the terms which upgrade the basic system and provide the compensations could be selectively added. This feature provided the capability of readily studying a number of system configurations. The composition of the six configurations studied is presented in table I. Configurations I and II are the basic and upgraded systems, respectively. Configurations III and IV are formed by incorporating the compensation for the existence of the disturbance torque during thrusting $1 + (|\lambda|/|\lambda_c|)$ into configurations I and II. Similarly, configurations V and VI are formed by adding the control-thrust-variation term t_ϵ to configurations III and IV. The delay time t_{dl} was included in all configurations. No attempt was made in the program to evaluate startup and decay lags in the thrustor. However, any such lags would have a negligible effect on the results for two reasons. First, the thrusting times were generally sufficiently large that the time constants typical of pneumatic thrustors would be negligible, and second, any difference between the actual and the desired vehicle deadband reentry rates that are caused by the lags would be compensated by the feedback term.

Each configuration was subjected to a range of sinusoidal disturbances given by

$$\lambda = \alpha\lambda_c \sin \omega_o t \qquad 0.01 \leq \alpha \leq 0.25 \tag{16}$$

and the number of thrustor firings and the total thrustor on time were recorded for each data run. In addition to the optimum system, a conventional on-off control system was subjected to the same disturbance environment and the data recorded for comparison purposes. All data runs were taken over four cycles of the disturbance function with the computer operating at 40 times real time. A summary of the model parameters used in the investigation is presented in table II.

RESULTS AND DISCUSSION

The pulsing frequency N_f, in pulses per year, as a function of the disturbance torque to control-torque ratio α, for each of the six configurations, is presented in figures 3(a) to (f), respectively. The results for the conventional on-off system and also the theoretical minimum for a constant disturbance torque to control-torque ratio equal to the root-mean-square value of α are presented in each figure for comparison. Figures 3(a) to (f) show that all configurations reduce the pulsing frequency from that of the conventional system to a value comparatively close to the theoretical minimum. The reduction is of the order of 10^6 pulses per year for an α of 0.25 and is greatest at the higher values of the distrubance torque. The reason for this is that, for the conventional system, the maximum angular excursion during coast becomes small as the disturbance torque increases, resulting in decreased coast times. As the configurations proceed from the simplest to the most complex, the pulsing-frequency curve generally approaches the theoretical minimum line. The deviation from the theoretical minimum for each configuration, expressed as a percentage of the theoretical minimum and averaged over the range of α, is presented in figure 4. The difference in performance between the basic system and the upgraded system can be seen by comparing the values for configurations I, III, and V in this figure with those for configurations II, IV, and VI, respectively. Calculating the average of the difference between these configurations shows that upgrading the system by including $\dot{\lambda}$ information results in an average drop in the deviation from the theoretical minimum pulsing frequency of 5.5 percent for the three cases.

The effect on the system performance of the incorporation of the term $1 + (|\lambda|/|\lambda_c|)$ to negate the effect of the disturbance torque during thrustor firing can be determined by comparing the results for configurations III and IV with those for configurations I and II, respectively, in figure 4. Calculating the average of these two cases shows a drop of 13.0 percent in the deviation when the term $1 + (|\lambda|/|\lambda_c|)$ is added. As would be expected, the effect of this term is more pronounced at the higher disturbance torque to control-torque ratios.

The effect of the feedback term t_ϵ can be shown by performing a similar comparison between the results for configurations V and VI, and III and IV. It is observed here, however, that the average percent deviation for configuration VI is larger than that for configuration IV. Reference to figure 3(f) shows that a large portion of the deviation is attributable to the two lowest values of α. If the deviations for these four configurations are averaged over the range of α from 0.05 to 0.25, the values become

Configuration	Average deviation, percent
III	10.7
IV	6.7
V	9.7
VI	2.0

Therefore, the effect of t_ϵ over the higher range of α is to reduce the average deviation by an average of 2.9 percent. Because no runs were made in this study in which the thrustor was changed, this reduction implies that, in this range, the feedback term corrects for lags in the system implementation between the calculation of the vehicle dynamic state and the time of thrust application. The reason for the relatively large deviations at low values of α for configuration VI is not fully understood. The only difference between configurations IV and VI is the addition of the term t_e. A survey of the computer data indicates that the backup system fires more often for these two cases than for the others, resulting in more total pulses. Since this occurs only when $\dot{\lambda}$ information and t_e are both present, the additional backup pulses may be caused by relatively large variations in t_e during the first few cycles of operation coupling with the larger change in λ during one-half cycle and producing higher rates at the deadband.

The total thrustor on time per year T_f as a function of the disturbance torque to control-torque ratio α is presented in figure 5 for all configurations. This parameter provides an indication of the relative fuel consumption for the various configurations. The fuel consumption is proportional to the duty cycle, that is, the ratio of thrust on time to total cycle time. In a soft limit cycle, the duty cycle is a function only of the disturbance torque to control-torque ratio, and since the six configurations operated in a soft limit cycle virtually all the time, little deviation was expected and obtained between configurations. Figure 5 also shows that T_f for the conventional system is quite close to that for the other systems, which indicates that the parameters chosen for this system allowed a transition to hard limit cycle operation at a disturbance-torque level well below the average value of the disturbance torque applied.

CONCLUSIONS

The analysis and computer study presented herein demonstrates the theoretical feasibility of a control logic system to provide the optimum phase-plane trajectory in the presence of time-varying disturbance torques. This system uses only the attitude error as input.

The types of systems investigated ranged from the simplest, which calculates the required thrustor on time from only the values of vehicle rate and acceleration at the deadband limit, to the most complicated, which also estimates the average disturbance acceleration over the following coast half-cycle and compensates for real or virtual changes in the control torque-to-inertia ratio. As the system is made more sophisticated, the deviation in thrustor pulsing frequency from the theoretical minimum decreases, with a drop of 18 percent from the simplest to the most complicated. The ratio of pulsing frequency for the conventional system to that for the optimum system for all configurations investigated was approximately 4 over the major portion of the disturbance-torque range. The improvement provided by the upgraded system over the equivalent system without information on the ratio of the rate of change of disturbance torque to inertia ($\dot{\lambda}$) amounts to an average drop of 5.5 percent in thrustor pulsing frequency. This difference may not warrant the inclusion of the $\dot{\lambda}$ information and the probable associated hardware complexity.

Lewis Research Center,
National Aeronautics and Space Administration,
Cleveland, Ohio, November 2, 1967,
125-19-03-03-22.

APPENDIX - OPTIMUM-LIMIT-CYCLE TRAJECTORY FOR VARIABLE CONTROL IMPULSE

For a given constant value of external disturbance torque, the idealized limit-cycle trajectory in the phase plane is shown in figure 6. The type of limit cycle traversed by the spacecraft depends on the magnitude of the angular impulse imparted to it during thrusting. For sufficiently small angular impulses, the opposite switching line will not be crossed, and the trajectory resembles path A. As the angular impulse is increased, the opposite switching line will eventually be contacted, and the vehicle traverses a path similar to B. It remains to be shown that path C is optimum from the standpoint of fuel consumption and number of thrustor firings.

For a specified period P, during which it is desired to control the spacecraft against a disturbance torque, the expressions for the total fuel required W and the total number of thrust pulses N_f are given by

$$W = \dot{w} d_a P \tag{A1}$$

$$N_f = \frac{d_a}{t_{on}} P \tag{A2}$$

where d_a is the duty cycle, or the ratio of thrusting time to total cycle time,

$$d_a = \frac{t_{on}}{t_{on} + t_{off}} \tag{A3}$$

For path A, as shown in figure 6, the duty cycle is given by

$$t_{on} = t_{01} = \frac{2\dot{\theta}_r}{\lambda_c - \lambda}$$

$$t_{off} = t_{10} = \frac{2\dot{\theta}_r}{\lambda}$$

Hence,

$$d_a = -\frac{\dfrac{2\dot{\theta}_r}{\lambda_c - \lambda}}{\dfrac{2\dot{\theta}_r}{\lambda_c - \lambda} + \dfrac{2\dot{\theta}_r}{\lambda}} = \frac{\lambda}{\lambda_c} \tag{A4}$$

Therefore, for path A,

$$\left.\begin{aligned} W &= \dot{w} d_a P \\ &= \frac{F}{I_{sp}}\left(\frac{\lambda}{\lambda_c}\right)P \\ &= \frac{P}{I_{sp}} \frac{J}{l} \lambda \end{aligned}\right\} \tag{A5}$$

and

$$\left.\begin{aligned} N_f &= \frac{P}{t_{01}}\left(\frac{\lambda}{\lambda_c}\right) \\ &= \frac{P\lambda}{2\dot{\theta}_r + t_{01}\lambda} \end{aligned}\right\} \tag{A6}$$

Hence, W is independent of the reentry angular rate $\dot{\theta}_r$, and N_f decreases as $\dot{\theta}_r$ increases, that is, tends to make the trajectory approach the opposite switching line.

For path B, the duty cycle is given by

$$d_a = \frac{t_{01} + t_{23}}{t_{01} + t_{23} + 2t_{12}} \tag{A7}$$

Also,

$$t_{01} = \frac{2\dot{\theta}_r}{\lambda_c - \lambda}$$

$$t_{12} = \frac{4\theta_d}{\dot{\theta}_r + \dot{\theta}'_r} \tag{A8}$$

and

$$t_{23} = \frac{2\dot{\theta}'_r}{\lambda_c + \lambda}$$

Hence, substituting equations (A8) into equation (A7) and collecting terms yield

$$d_a = \frac{\dot{\theta}_r^2(\lambda_c + \lambda) + 2\dot{\theta}_r\dot{\theta}'_r\lambda_c + \dot{\theta}'^2_r(\lambda_c - \lambda)}{\dot{\theta}_r^2(\lambda_c + \lambda) + 2\dot{\theta}_r\dot{\theta}'_r\lambda_c + \dot{\theta}'^2_r(\lambda_c - \lambda) + 4\theta_d\left(\lambda_c^2 - \lambda^2\right)} \tag{A9}$$

but

$$\dot{\theta}'_r = \sqrt{\dot{\theta}_r^2 - 4\theta_d\lambda}$$

from which

$$d_a = \frac{\dot{\theta}_r^2\lambda_c + \dot{\theta}_r\lambda_c\sqrt{\dot{\theta}_r^2 - 4\theta_d\lambda} - 2\theta_d\lambda(\lambda_c - \lambda)}{\dot{\theta}_r^2\lambda_c + \dot{\theta}_r\lambda_c\sqrt{\dot{\theta}_r^2 - 4\theta_d\lambda} + 2\theta_d\lambda_c(\lambda_c - \lambda)} \tag{A10}$$

Note that for values of $\dot{\theta}_r$ less than $\sqrt{4\theta_d\lambda}$, the trajectory resembles path A, and for $\dot{\theta}_r$ greater than $\sqrt{4\theta_d\lambda}$, the path resembles B. Now define a parameter γ by

$$\gamma = \frac{\dot{\theta}_r^2}{4\theta_d\lambda} \tag{A11}$$

Substituting this parameter into equation (A10) yields

$$d_a = \frac{\gamma + \sqrt{\gamma(\gamma - 1)} - \frac{1}{2}\left(1 - \frac{\lambda}{\lambda_c}\right)}{\gamma + \sqrt{\gamma(\gamma - 1)} + \frac{1}{2}\left(\frac{\lambda_c}{\lambda} - 1\right)} \tag{A12}$$

The final terms in both numerator and denominator are constant. Let

$$\frac{1}{2}\left(1 - \frac{\lambda}{\lambda_c}\right) = k_1$$

$$\frac{1}{2}\left(\frac{\lambda_c}{\lambda} - 1\right) = k_2$$

hence,

$$d_a = \frac{\gamma + \sqrt{\gamma(\gamma - 1)} - k_1}{\gamma + \sqrt{\gamma(\gamma - 1)} + k_2}$$

Taking the derivative of d_a with respect to γ and collecting terms yield

$$\frac{d(d_a)}{d\gamma} = \frac{\left[1 + \frac{1}{2}\left(\gamma^2 - \gamma\right)^{-1/2}(2\gamma - 1)\right]}{\left[\gamma + \left(\gamma^2 - \gamma\right)^{1/2} + k_2\right]^2}(k_1 + k_2) \tag{A13}$$

Now,

$$k_2 + k_1 = \frac{1}{2}\left(1 - \frac{\lambda}{\lambda_c}\right) + \frac{1}{2}\left(\frac{\lambda_c}{\lambda} - 1\right) = \frac{1}{2}\left(\frac{\lambda_c}{\lambda} - \frac{\lambda}{\lambda_c}\right)$$

Therefore, $k_1 + k_2$ is always positive for $\lambda_c > \lambda$. The other terms in brackets in equation (A13) are always positive for values of γ greater than 1. Hence, $d(d_a)/d\gamma$ is always positive for any path B, and, therefore, d_a increases as γ increases. Since both W and N_f are directly proportional to d_a, both of these quantities increase as the angular impulse increases.

In summary, for trajectories similar to path A, the fuel requirement remains constant, and the number of thrust pulses increases as the angular impulse decreases. For those trajectories of type B, both the fuel required and the number of thrust pulses increase as the angular impulse increases. It, therefore, follows that path C must be optimum from the standpoint of the fuel required and the total number of thrust pulses.

TABLE I. - COMPOSITION OF VARIOUS CONFIGURATIONS STUDIES

Additive Term	Configuration					
	I	II	III	IV	V	VI
Spacecraft angular rate, $\dot{\theta}$	X	X	X	X	X	X
Ratio of disturbance torque to moment of inertia, λ	X	X	X	X	X	X
Rate of change of disturbance torque to inertia ratio with time, $\dot{\lambda}$	---	X	---	X	---	X
Compensation for existence of disturbance torque during thusting, $1 + (\lvert\lambda\rvert / \lvert\lambda_f\rvert)$	---	---	X	X	X	X
Thrust-variation compensation time, t_ϵ	---	---	---	---	X	X

TABLE II. - SPACECRAFT MODEL PARAMETERS

(a) Optimum system

Control torque-to-inertia ratio, λ_c, rad/sec^2	3.49×10^{-5}
Primary deadband limit, θ_d, rad	8.73×10^{-3}
Backup deadband limit, θ_b, rad	1.31×10^{-2}
Primary hysteresis, h_d, rad	4.36×10^{-4}
Backup hysteresis, h_b, rad	4.36×10^{-4}
Angular measurement interval, $\Delta\theta$, rad	1.75×10^{-3}
Maximum angular excursion, θ_{max}, rad	1.58×10^{-2}
Fixed thrustor time delay, t_{dl}, sec	1.0
Thrustor compensation weighting constant, k_ϵ	0.2
Orbital angular velocity, ω_o, rad/sec	1.05×10^{-3}

(b) Conventional system

Control torque-to-inertia ratio, λ_c, rad/sec^2	3.49×10^{-5}
Deadband limit, θ_d, rad	8.73×10^{-3}
Hysteresis, h, rad	4.36×10^{-4}
Lead time constant, τ_1, sec	8.1
Lag time constant, τ_2, sec	1.0
Zero-torque duty cycle, percent	0.83
Zero-torque thrust on time, sec	2.88
Orbital angular velocity, ω_o, rad/sec	1.05×10^{-3}

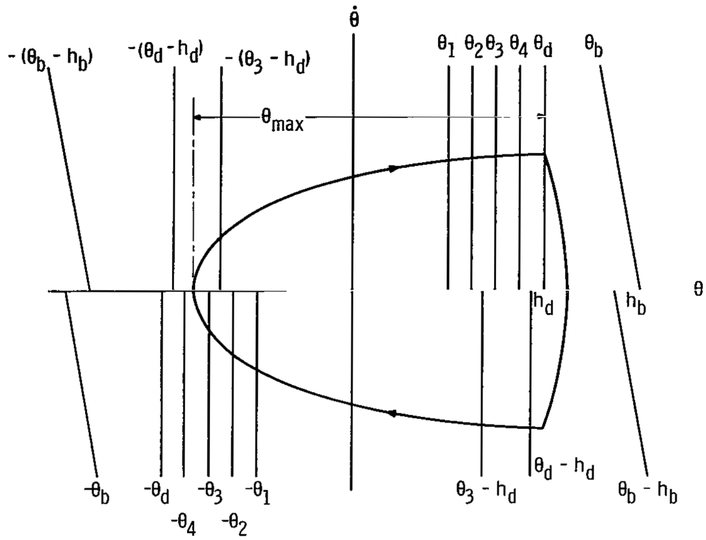

$t_0 = t_{(\theta_3 - h_d)} - t_{(\theta_d - h_d)}$

$t_1 = t_{\theta_3} - t_{\theta_1}$

$t_2 = t_{\theta_4} - t_{\theta_2}$

$t_3 = t_{\theta_d} - t_{\theta_3}$

$\Delta\theta = (\theta_3 - \theta_1) = (\theta_4 - \theta_2) = (\theta_d - \theta_3)$

$= (\theta_d - h_d) - (\theta_3 - h_d)$

$\dot{\theta}_0 = \Delta\theta/t_0 \qquad \dot{\theta}_2 = \Delta\theta/t_2$

$\dot{\theta}_1 = \Delta\theta/t_1 \qquad \dot{\theta}_3 = \Delta\theta/t_3$

Figure 1. - Phase-plane representation of optimum control system operation.

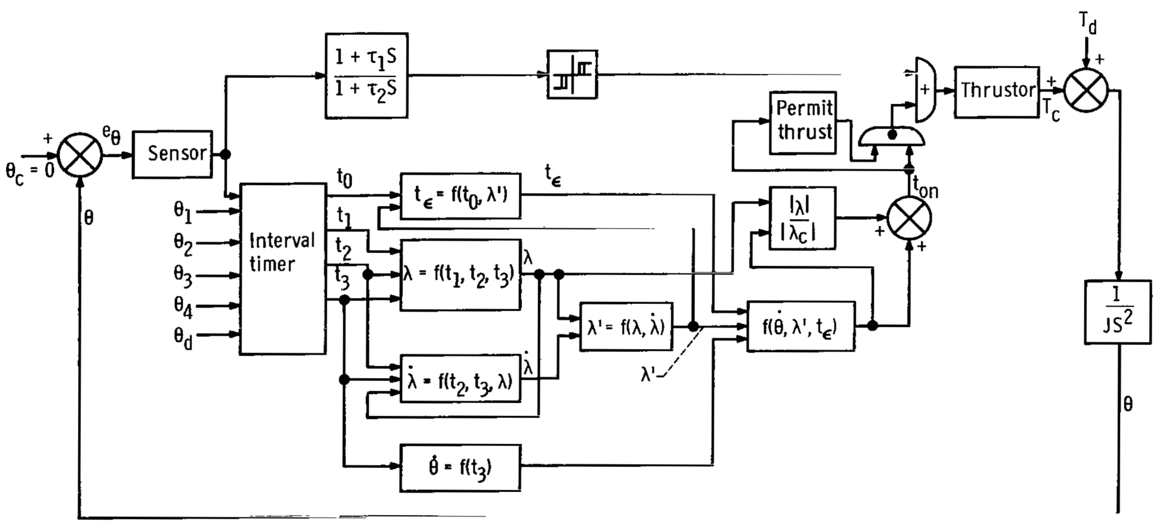

Figure 2. - Control system.

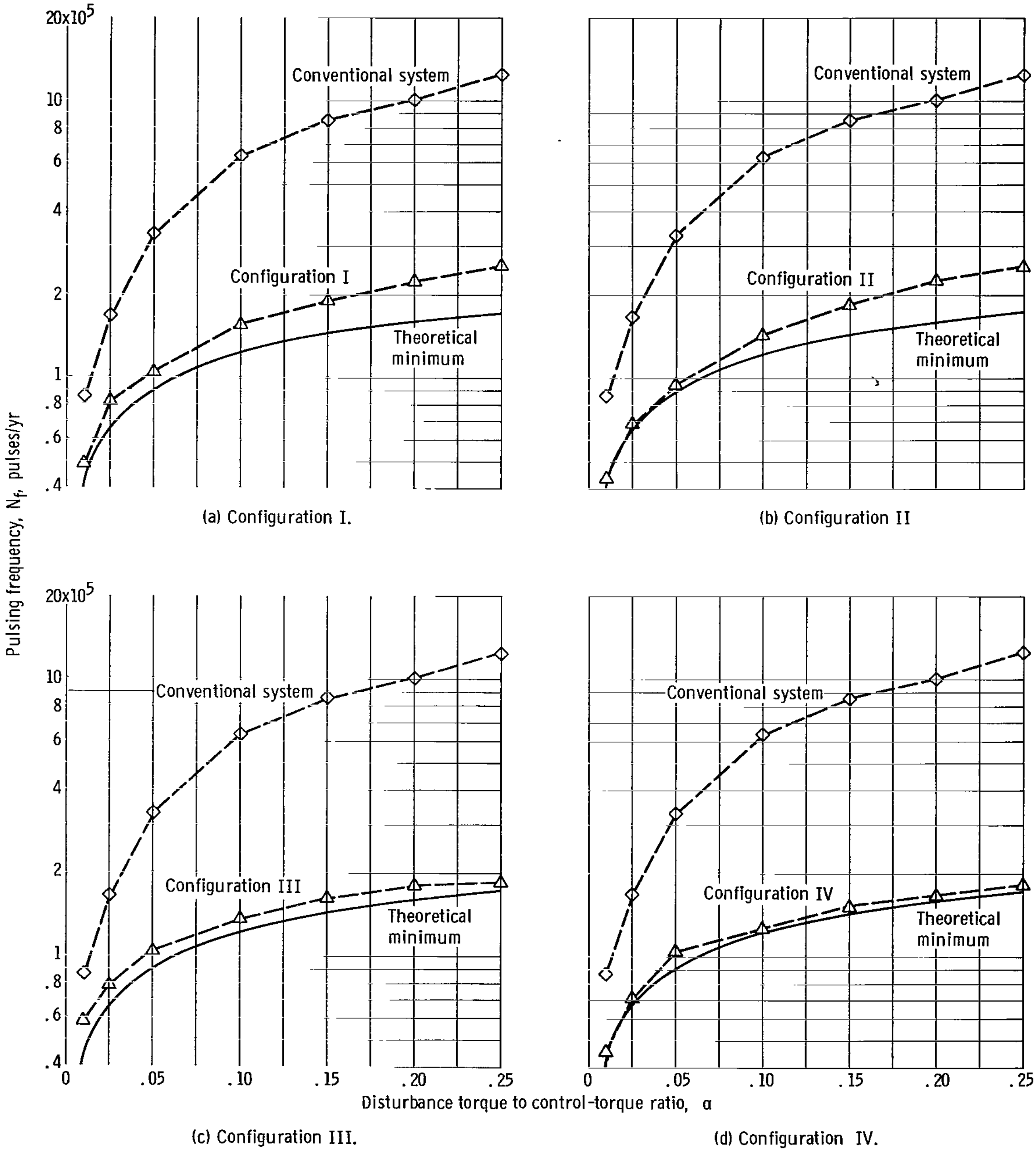

Figure 3. - Pulsing frequency as function of disturbance torque to control-torque ratio.

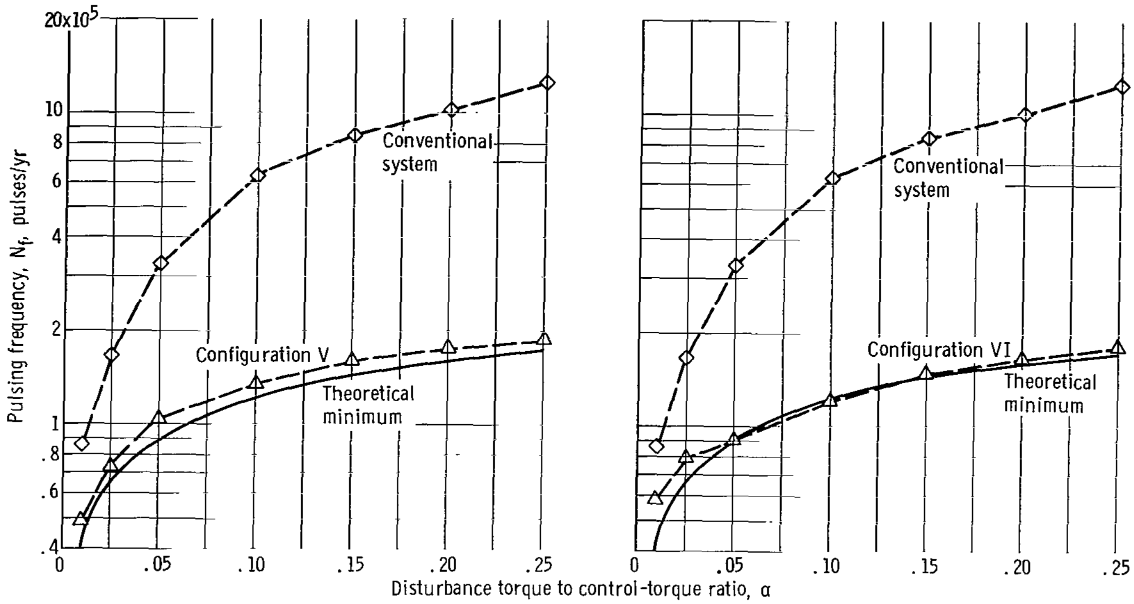

(e) Configuration V. (f) Configuration VI.

Figure 3. - Concluded.

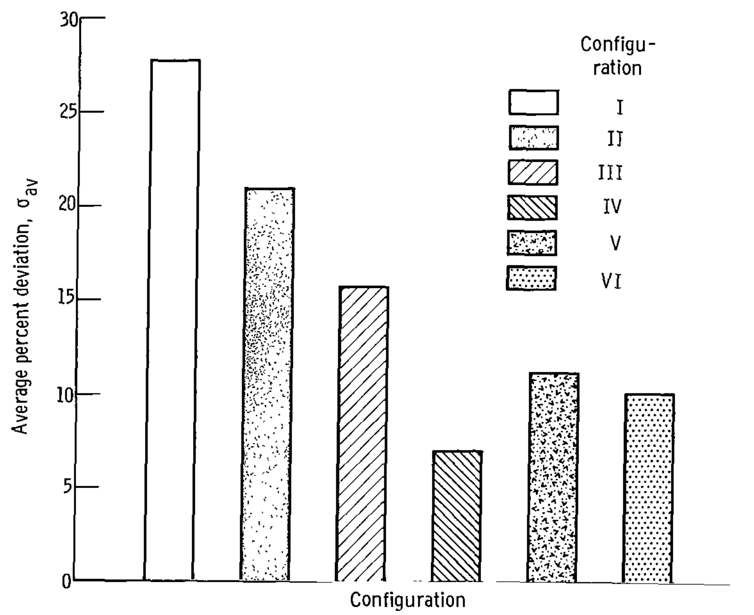

Figure 4. - Average percent deviation from minimum pulsing frequency for each configuration.

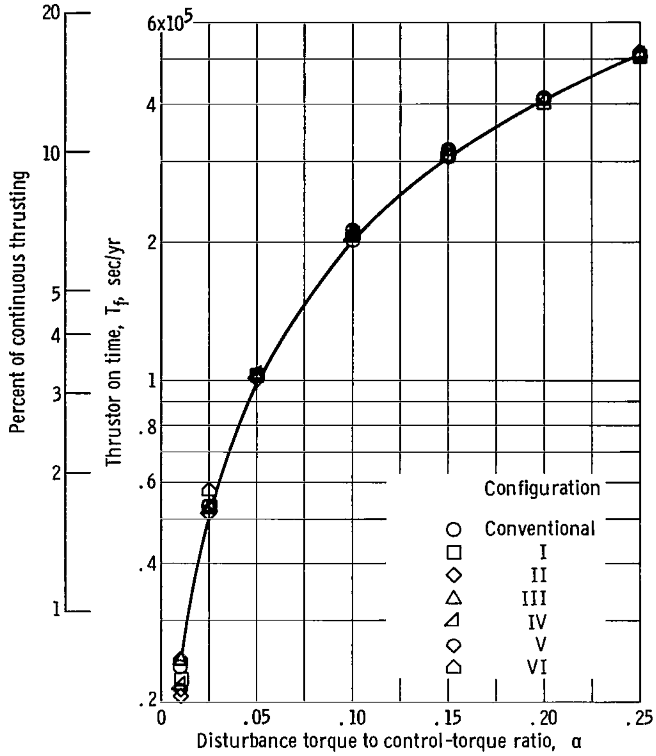

Figure 5. - Thrustor on time as function of disturbance torque to control-torque ratio for all configurations and conventional system.

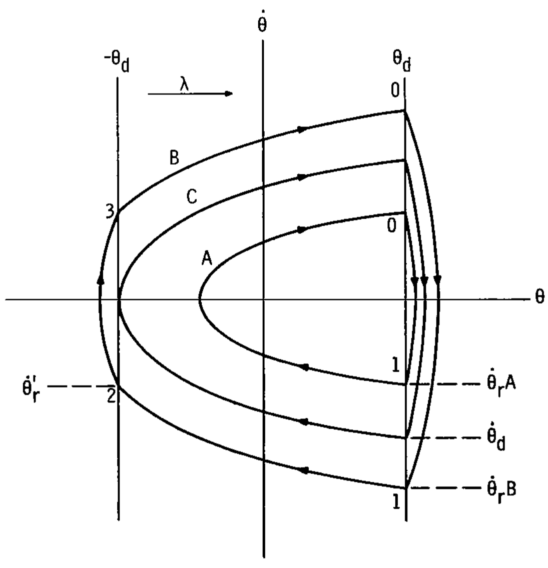

Figure 6. - Variation of form of phase-plane trajectory with vehicle angular rate at thrustor shutoff.

National Aeronautics and Space Administration
WASHINGTON, D. C.

OFFICIAL BUSINESS

FIRST CLASS MAIL

POSTAGE AND FEES PAID
NATIONAL AERONAUTICS AND
SPACE ADMINISTRATION

10U 001 56 51 3DS 68092 00903
AIR FORCE WEAPONS LABORATORY/AFWL/
KIRTLAND AIR FORCE BASE, NEW MEXICO 87117

POSTMASTER: If Undeliverable (Section 158 Postal Manual) Do Not Return

"The aeronautical and space activities of the United States shall be conducted so as to contribute . . . to the expansion of human knowledge of phenomena in the atmosphere and space. The Administration shall provide for the widest practicable and appropriate dissemination of information concerning its activities and the results thereof."

—NATIONAL AERONAUTICS AND SPACE ACT OF 1958

NASA SCIENTIFIC AND TECHNICAL PUBLICATIONS

TECHNICAL REPORTS: Scientific and technical information considered important, complete, and a lasting contribution to existing knowledge.

TECHNICAL NOTES: Information less broad in scope but nevertheless of importance as a contribution to existing knowledge.

TECHNICAL MEMORANDUMS: Information receiving limited distribution because of preliminary data, security classification, or other reasons.

CONTRACTOR REPORTS: Scientific and technical information generated under a NASA contract or grant and considered an important contribution to existing knowledge.

TECHNICAL TRANSLATIONS: Information published in a foreign language considered to merit NASA distribution in English.

SPECIAL PUBLICATIONS: Information derived from or of value to NASA activities. Publications include conference proceedings, monographs, data compilations, handbooks, sourcebooks, and special bibliographies.

TECHNOLOGY UTILIZATION PUBLICATIONS: Information on technology used by NASA that may be of particular interest in commercial and other non-aerospace applications. Publications include Tech Briefs, Technology Utilization Reports and Notes, and Technology Surveys.

Details on the availability of these publications may be obtained from:

SCIENTIFIC AND TECHNICAL INFORMATION DIVISION

NATIONAL AERONAUTICS AND SPACE ADMINISTRATION

Washington, D.C. 20546